Cell Cycle 12:18, 3037–3051; September 15, 2013; © 2013 Landes Bioscience

E2F-7 couples DNA damage-dependent transcription with the DNA repair process

Lykourgos-Panagiotis Zalmas[1], Amanda S Coutts[1], Thomas Helleday[2], and Nicholas B La Thangue[1,*]

[1]Laboratory of Cancer Biology; Department of Oncology; University of Oxford; Oxford, UK; [2]Science for Life Laboratory; Department of Medical Biochemistry and Biophysics;Karolinska Institute; Stockholm, Sweden

Keywords: E2F, transcription, DNA damage, DNA repair, somatic mutation

The cellular response to DNA damage, mediated by the DNA repair process, is essential in maintaining the integrity and stability of the genome. E2F-7 is an atypical member of the E2F family with a role in negatively regulating transcription and cell cycle progression under DNA damage. Surprisingly, we found that E2F-7 makes a transcription-independent contribution to the DNA repair process, which involves E2F-7 locating to and binding damaged DNA. Further, E2F-7 recruits CtBP and HDAC to the damaged DNA, altering the local chromatin environment of the DNA lesion. Importantly, the E2F-7 gene is a target for somatic mutation in human cancer and tumor-derived mutant alleles encode proteins with compromised transcription and DNA repair properties. Our results establish that E2F-7 participates in 2 closely linked processes, allowing it to directly couple the expression of genes involved in the DNA damage response with the DNA repair machinery, which has relevance in human malignancy.

Introduction

Double-strand breaks (DSBs) are the most dangerous forms of DNA damage, thus their faithful repair is essential for the maintenance of genomic integrity and cell survival.[1] To protect against the harmful effects of DSBs, cells employ a network of biochemical cascades, termed DNA damage checkpoints, which are responsible for detecting and translating DNA damage signals into a cellular response that prevents propagation and segregation of damaged DNA.[2]

DSB repair is achieved by the error-prone non-homologous end joining (NHEJ) and the error-free homologous recombination (HR). While NHEJ occurs primarily during the G_0/G_1 phases of the cell cycle, HR occurs during the S/G_2 phases, where an intact sister chromatid is used as a repair template.[3] HR is initiated by the assembly of DNA repair proteins to the DSB after recognition by PI3K-like kinases, which phosphorylate the H2A variant H2AX (γH2AX).[4] In turn, γH2AX signals the recruitment of the MRE11–RAD50–NBS1 (MRN) complex, which promotes DSB resection and creates long stretches of single-stranded DNA (ssDNA), which are then coated with replication-protein A (RPA) and serve as a scaffold for the recruitment of the RAD51 recombinase and other accessory proteins to complete the repair of damaged DNA.[5]

The E2F family is a group of transcription factors that regulate cell cycle, apoptosis, and differentiation.[6] The founding member, E2F-1, is a key target for the retinoblastoma tumor suppressor protein pRb, which regulates E2F-1 activity.[7,8] The E2F-7 subunit is an unusual member of the E2F family, whose DNA binding activity does not require association with a DP partner and acts as a transcriptional repressor independently of binding to pRb family proteins.[9,10] Instead, E2F-7 utilizes 2 tandemly arranged DNA binding domains that enable efficient binding to E2F sites.[9-11] During the DNA damage response, E2F-7 is upregulated, suppressing transcription and DNA damage-induced apoptosis.[12]

Here, we have examined whether E2F-7 performs a non-transcriptional role in DNA damaged cells. We provide evidence that E2F-7 makes a transcription-independent contribution to the DNA repair process, which requires it to locate to the site of damaged DNA. E2F-7 recruits CtBP and HDAC, which alters the chromatin environment of the damaged DNA. Significantly, the E2F-7 gene is a target for somatic mutation in cancer, which results in mutant proteins that exhibit compromised transcription and DNA repair properties. Thus, by coupling transcription with DNA repair E2F-7 makes an important contribution to DNA repair, and this process has significance in human cancer.

Results

E2F-7 influences the cellular response during DNA repair

The regulation of E2F-7 upon DNA damage[12] prompted us to examine the biological role of E2F-7 during the DNA damage response. To distinguish between DNA damage-induced apoptosis and repair, we depleted cells of E2F-7, treated them with a non-lethal yet DNA damage-inducing dose of camptothecin (CPT;25 nM),[13,14] and released them into drug-free medium (**Fig. 1A**).

*Correspondence to: Nicholas B La Thangue; Email: nick.lathangue@oncology.ox.ac.uk
Submitted: 08/05/2013; Accepted: 08/07/2013
http://dx.doi.org/10.4161/cc.26078

Exposure to CPT increased the level of the DNA damage sensor γH2AX, which subsequently began to decline by 6 h; a parallel stabilization of E2F-7 occurred, which began to decline at 8 h (**Fig. 1A**).[15] In the absence of E2F-7, γH2AX levels were greater and remained elevated over a longer time period than in the control NT siRNA-treated cells (**Fig. 1A**, i); this effect was also apparent by immunostaining, where typical γH2AX foci were apparent (**Fig. 1A**, ii). It is noteworthy that depletion of E2F-7 in the absence of DNA damage was not sufficient to affect γH2AX (**Fig. 1A**, i), indicating that the influence of E2F-7 on γH2AX occurred independently of the increased expression of E2F target genes.

Under normal culture conditions, the absence of E2F-7 had minimal effect on the cell cycle (**Fig. 1B**, i). However, in response to DNA damage, the size of the G_2/M phase cell population was clearly affected by the absence of E2F-7 (38% compared with 30% in the control cells), and fewer cells were evident in G_1/S phase (**Fig. 1B**, i; **Fig. S1**). Furthermore, the loss of E2F-7 did not cause any substantial perturbation in DNA synthesis, as BrdU incorporation in cells pulse-labeled prior to CPT treatment and then chased in BrdU-free medium,remained relatively constant throughout the time of analysis (**Fig. 1B**, ii; **Fig. S1**). In contrast, when cells were labeled with BrdU post-CPT treatment, as a means to investigate the effect of E2F-7 specifically during DNA repair, BrdU incorporation in the E2F-7 siRNA treated cells was initially delayed but by 8 h was greater than the control treatment (**Fig. 1C**; **Fig. S1**). These results are consistent with the increased G_2/M phase population upon E2F-7 depletion compared with the control NT siRNA treatment (**Fig. 1B**, i), suggesting that a greater number of cells had traversed S phase and entered G_2/M phase, especially at the later stages of the repair process. Overall, the results indicate that E2F-7 impacts on DNA repair (DSBs are repaired more slowly, reflected in elevated and extended γH2AX level in E2F-7-depleted cells) and DNA synthesis (more cells progressed through S phase into G_2/M and enhanced BrdU incorporation in E2F-7-depleted cells).

E2F-7 is a regulator of the DNA repair process

The influence of E2F-7 on γH2AX, together with the implication that DNA repair was under aberrant control, prompted us to examine the role of E2F-7 in HR, which is the prominent DNA repair process taking place in S/G_2 phase cells.[16] We used the DR-GFP reporter system,[17] where site-specific DNA repair is induced by ISceI endonuclease-driven DSB formation within the reporter GFP gene, and repair by HR results in the reconstitution of full-length GFP gene, which gives rise to GFP-positive cells (**Fig. 2A**; **Fig. S2**).

Cells treated with E2F-7 siRNA and transfected with ISceI showed a marked increase in GFP, reflecting an increase in HR compared with control treated cells (**Fig. 2B**). As expected, HR was abolished upon depletion of RAD51 (**Fig. 2B**; **Fig. S2**), which is essential for HR.[18] The effect of depleting E2F-7 was also apparent at increased levels of ISceI (**Fig. S2**). Importantly, depletion of E2F-1 similarly increased GFP, although to a lesser extent (**Fig. S2**), suggesting that the effect of E2F-7 depletion was not linked to upregulation of E2F-1. Conversely, expressing ectopic E2F-7 protein resulted in a decrease in the GFP signal and the effect on HR was dependent on the integrity of its DNA binding and dimerization domains (mutated in DBD and DD, respectively; **Fig. 2C**). Further, ectopic E2F-8 failed to affect the GFP signal (**Fig. S2**), indicating that the role of E2F-7 in HR is not shared with its closely related family member E2F-8.

Although E2F-7 did not influence DNA damage in the absence of CPT (**Fig. 1A**), it was important to test whether the effect of E2F-7 on HR, apparent in the DR-GFP assay, resulted from a transcription-dependent or -independent mechanism. We found that the RNA level of the recombining GFP locus (**Fig. 2A and D**) did not change in E2F-7 expressing cells in both the presence and absence of ISceI (**Fig. 2E**). Further, analysis of the DNA sequence of the DR-GFP cassette did not identify any canonical E2F binding motifs, and when discrete DNA regions of the DR-GFP cassette were cloned into a luciferase reporter vector (**Fig. 2D**), E2F-7 failed to affect reporter activity, in contrast to the effect on E2F-1 promoter-luciferase (**Fig. 2F**).[9,12] Thus, the absence of any notable change in GFP RNA levels and of cryptic E2F-7 promoter sites argues against a direct transcription effect of E2F-7 on the DR-GFP cassette.

E2F-7 is recruited to the double strand break and binds to damaged DNA

We reasoned that E2F-7 may make direct contact with the DNA of the DR-GFP cassette and examined this possibility by chromatin immunoprecipitation (ChIP), where E2F-7-bound chromatin was immunoprecipitated and the position of binding assessed by PCR using specific primers (**Fig. 2D**). E2F-7 was detected upstream the ISceI-cleavage site (Isc site), which was apparent only upon expression of ISceI at 8 to 16 h (**Fig. 3A**). In contrast, E2F-7 constitutively bound to the E2F-1 promoter under the same conditions (**Fig. S3**). The specificity of the ChIP signal was confirmed by depleting E2F-7 with siRNA (**Fig. 3A**; **Fig. S3**). Further, binding to the Isc site required the integrity of its dimerization and DNA binding domains (**Fig. 3B**) and thus paralleled the effects seen in the HR assay (**Fig. 2C**). Significantly, when cells were microirradiated with UV irradiation,[19] E2F-7 localized to DSBs and colocalized with γH2AX and 53BP1 (**Fig. 3C**). The co-localization of E2F-7 with proteins directly involved in DNA repair (γH2AX and 53BP1)[20-22] combined with the ChIP analysis (**Fig. 3A**) suggests that E2F-7 locates to and binds to areas of damaged DNA.

To substantiate the role of E2F-7 at DSBs, we evaluated by electrophoretic mobility shift assay (EMSA) whether E2F-7 can bind directly to 5′ overhang, 3′ overhang or blunt end DNA probes (**Fig. 3D**) that resemble DNA structures that occur during DSB processing.[23] As expected, binding of purified His-tagged E2F-7 (**Fig. 3D**, ii–iv) to an E2F binding site derived from the E2F-1 promoter was evident (**Fig. 3E**, i; **Fig. S3**). E2F-7 could also bind to the 5′ and 3′ overhang and blunt end DNA structures (**Fig. 3E**, ii–iv). The addition of His antibody shifted the E2F-7: DNA complexes (**Fig. 3E**) and an E2F-7 derivative that lacked the second DBD (ΔDBD2) failed to bind (**Fig. S3**). Thus, E2F-7 localizes to chromatin regions where DSBs occur and has the intrinsic capacity to bind to the type of DNA structures that occur during the HR process.

E2F-7 requires association with CtBP to regulate HR

Having established that the integrity of E2F-7 DNA binding and dimerization domains was important for its HR activity

(**Fig. 2C**), it was of interest to explore whether other regions of the protein could influence its activity. To this end, we generated C-terminal deletion mutants (Δ1 to Δ4; **Fig. 4A**) and compared their activity in transcription and DR-GFP reporter assays. All mutants were able to repress transcription of the E2F-1 promoter, in contrast to the DBD and DD mutants, which, as previously

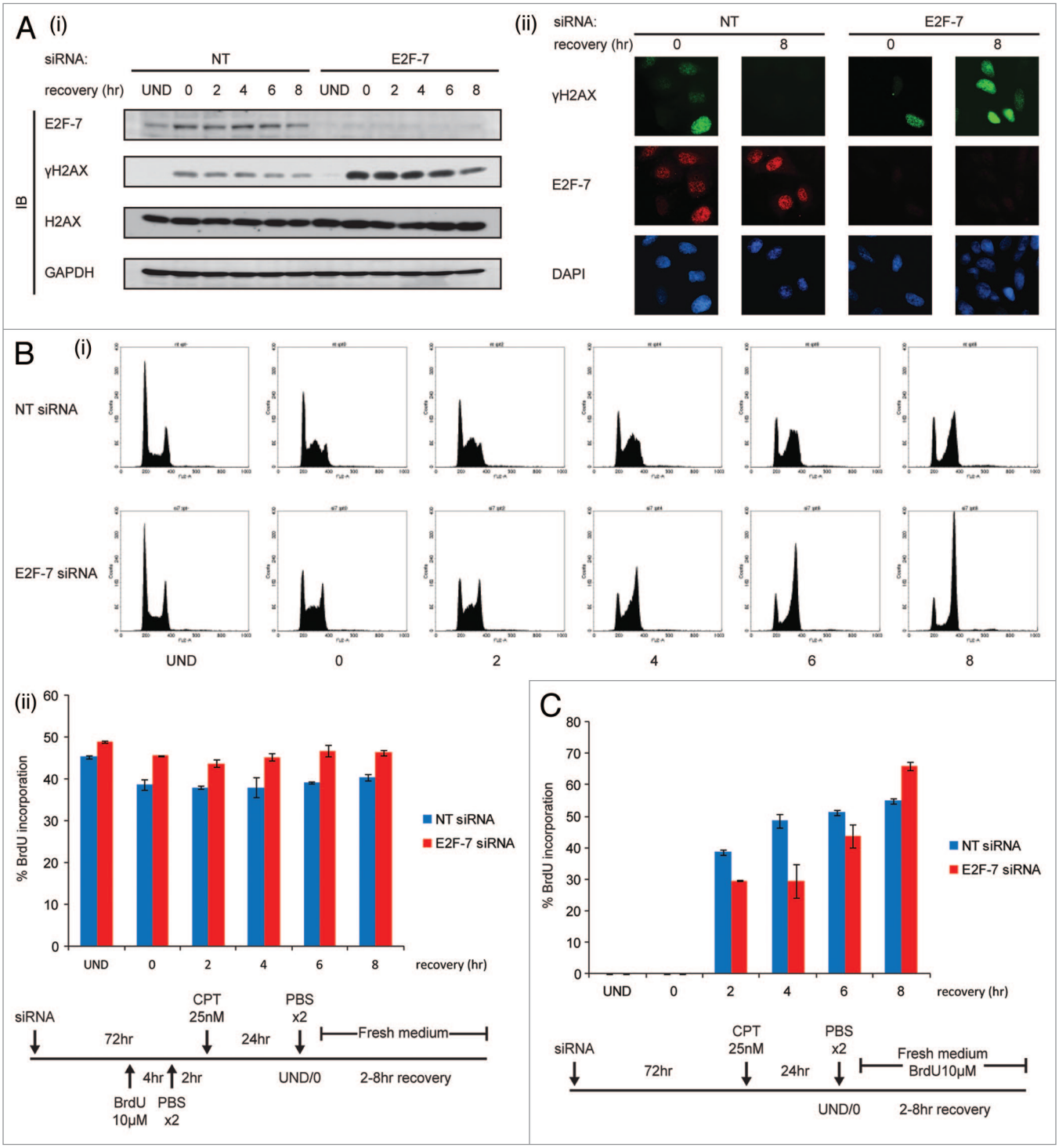

Figure 1. E2F-7 regulates the cellular response during DNA repair. (**A**) (i) U2OS cells were treated with NT or E2F-7 siRNA and subjected to camptothecin (CPT; 25 nM) treatment or left untreated (UND) for 16 h, washed, and allowed to recover in drug-free media, as indicated. H2AX phosphorylation (γH2AX) was analyzed by immunoblotting against total H2AX levels; GAPDH served as a loading control. (ii) U2OS cells were treated as in (i) and γH2AX was monitored by indirect immunofluorescence. Cell nuclei were counter-stained with DAPI. (**B**) (i) U2OS cells were treated as in (**A**) and cell cycle profiles analyzed by flow cytometry. See also **Figure S1A**, i and ii. (ii) BrdU incorporation analysis (%) in NT and E2F-7 siRNA treated cells at the indicated times, data represent the means of three replicates. See also **Figure S1A**, iii. (**C**) BrdU incorporation analysis (%) of U2OS cells, treated as in (**a**), where cells were continuously labeled with BrdU (10 μM) after removal of CPT. See also **Figure S1B**.

reported, failed to do so (**Fig. 4B**, i; **Fig. S4**).[12] However, the C-terminal deletion mutants had reduced effects in the HR assay, exhibiting similar activity to the DBD and DD mutants (**Fig. 4B**, ii). As the C-terminal region is dispensable for its transcription effects, these results reinforce the transcription-independent role of E2F-7 in HR and highlight the importance of the C-terminal region.

In exploring the mechanism involved, we looked for motifs in E2F-7 that informed on potential interaction partners and identified a binding site for the CtBP protein (**Fig. 4C**, i), an established co-repressor for a variety of transcriptional repressors.[24] Indeed, an interaction between E2F-7 and CtBP was apparent in cells under DNA damage conditions (**Fig. 4C**, ii). A loss-of-function E2F-7 deletion mutant (E2F-7ΔCtBP; **Fig. 4C**, i; **Fig. S4**) retained the ability to repress transcription (**Fig. 4D**; **Fig. S4**) but failed to affect HR activity in the DR-GFP reporter system compared with E2F-7 (**Fig. 4E**; **Fig. S4**; 90% reduced activity). Significantly, CtBP could be detected by ChIP analysis on the Isc site of the DR-GFP locus, and its presence was dependent on E2F-7 (**Fig. 4F**; **Fig. S4**). Together, these results indicate that the CtBP-binding motif in E2F-7 influences HR in the DR-GFP reporter assay and implicate CtBP in the HR process.

E2F-7 influences chromatin acetylation at the site of recombination

Since CtBP can exist in a complex with chromatin modifying HDAC subunits,[24,25] we tested for the presence of HDAC subunits in the E2F-7 complex and identified both HDAC1 and 2 (**Fig. 5A**). By ChIP analysis, both HDAC subunits were detected at the Isc site of the DR-GFP locus, and their presence was dependent on E2F-7 (**Fig. 5B**; **Fig. S4**).

The association of HDAC with E2F-7 prompted us to evaluate the level of histone acetylation at the GFP locus by ChIP analysis. Upon depletion of E2F-7, there was a considerable increase (4-fold) in acetylation upstream of the Isc site ("up" site, **Fig. 2D**), which was dependent on ISceI and not apparent at the other DNA sites tested (**Fig. 5C**). In contrast, the level of other chromatin modifications (H3K4me3 and H3K27me3) and heterochromatic chromatin marks (H3K9me3) remained largely unchanged (**Fig. 5C**). These results suggest that E2F-7, through recruitment of chromatin modifiers like HDAC, regulates the acetylation of chromatin around the recombining GFP locus.

Tumor mutations in human cancer

We were interested to evaluate the importance of the properties ascribed to E2F-7 here, in human cancer. We therefore interrogated the Catalogue of Somatic Mutations in Cancer (COSMIC) database and identified a number of somatic mutations in the E2F-7 gene (28 total: 24 missense and 4 nonsense; **Fig. 6A**), supported by the absence of the mutation in normal matched tissue.

We sought to determine the functional relevance of the mutations in the context of transcriptional repression and HR by E2F-7, based on the premise that, if the properties of E2F-7 were important for its normal biological role, then we might expect them to be aberrant in tumor-derived mutants. With the exception of the C-terminal truncation R288* and R333*, where one of the DNA binding and dimerization domains is truncated, all the other E2F-7 mutants were able to undergo nuclear accumulation and dimerize with E2F-7 (**Fig. 6B and C**). We evaluated the activity of the mutant derivatives on transcription, when co-expressed with E2F-1, an assay previously used to assess E2F-7 repression activity[12] (**Fig. 6D**). In comparison to wild-type E2F-7 and the DBD mutant, which retain and lack repression activity, respectively, the missense derivatives displayed modest differences in their ability to repress, with the exception of R185H, which carries a mutation in a residue essential for DNA binding (**Fig. 6A**). Notably, the E2F-7 truncations derived from nonsense mutations exhibited impaired ability to repress, particularly in the case of R288* and R333* (**Fig. 6D**; **Fig. S5**). When the mutants were evaluated in the DR-GFP assay, a general coincidence between the effect on HR and transcription was apparent; the E2F-7 truncations in particular exhibited compromised activity compared with the wild-type E2F-7 (**Fig. 6E**; **Fig. S5**). Further, R185H failed to affect HR activity to the same extent as wild-type E2F-7 (**Fig. 6E**). These results therefore suggest that the functional properties that have been ascribed to E2F-7 are affected by mutation in human cancer.

Discussion

Cells depleted of E2F-7 exhibit an aberrant DNA damage response in the extended time that γH2AX (an early response to DNA double-strand breaks) is detected, suggesting failure to efficiently repair DSBs. There was also a reduced number of cells in S phase and concomitant increase in G_2/M phase. These results are consistent with the idea that E2F-7 performs a role in the DNA repair process. Indeed, using the DR-GFP assay to measure the effect of E2F-7 in HR, we found that E2F-7 regulates HR activity. Further, E2F-7 can co-localize with γH2AX and 53BP1 in DNA damaged cells, bind directly to the recombining DNA, and, importantly, interact and recruit accessory factors, including

Figure 2 (See opposite page). E2F-7 regulates HR. (**A**) Schematic representation of the DR-GFP cassette, where expression of ISceI endonuclease cleaves its recognition site to generate a DSB. The second copy of the GFP gene (iGFP) acts as a template for DNA repair. GFP is expressed only after repair by HR. (**B**) U2OS DR-GFP cells were transfected with NT, E2F-7 or RAD51 siRNA and control vector (–) or ISceI (+). Shown are normalized GFP levels. Error bars, SD (n = 3). Statistical analysis by unpaired *t* test (***$P \leq 0.001$). See also **Figure S2B**. (**C**) U2OS DR-GFP cells were co-transfected with control vector (–) or ISceI (+) and E2F-7 (7), dimerization domain (7DD) or DNA-binding domain (7DBD) mutant. Shown are normalized GFP levels. Error bars, SD (n = 3). Statistical analysis by unpaired *t* test ($_{***} = P \leq 0.001$, $_{**} = P \leq 0.01$). See also **Figure S2F**. (**D**) Schematic representation of the DR-GFP cassette, indicating the position of GFP RNA and ChIP primers designed against sequences that are not shared between SceGFP and iGFP, ensuring amplification only of the SceGFP locus. (**E**) RNA extracted from U2OS DR-GFP cells, transfected with control vector (–) or HA-ISceI (+) and E2F-7 (7), 7DBD or ΔCtBP mutant (7ΔCt) were subjected to RT-PCR with primers that amplify a SceGFP sequence only, for the indicated number of cycles (25 or 30). 18S rRNA serves as loading control. (**F**) U2OS DR-GFP cells were co-transfected with vector (v) or E2F-7 (7), together with DNA fragments of the DR-GFP cassette (up, Isc, thru, down; **Fig. 2D**); E2F-1-luciferase reporter served as a positive control for the transcription effects of E2F-7, and CMV-β-gal as the internal control for transfection efficiency. Transcriptional activity was assessed by luciferase reporter assay and the results represent the ratio of luciferase to β-gal activity. See also **Figure S2G**.

CtBP and HDAC1 and 2, to the DSB. Our results therefore are consistent with the idea that E2F-7 contributes through both transcriptional and non-transcriptional mechanisms to the DNA repair process (**Fig. 6F**).

Multiple relationships between transcription and DNA repair proteins have been previously reported in eukaryotic cells. For example, certain subunits of transcription factor TFIIH are involved with nucleotide excision repair,[26] and transcriptional

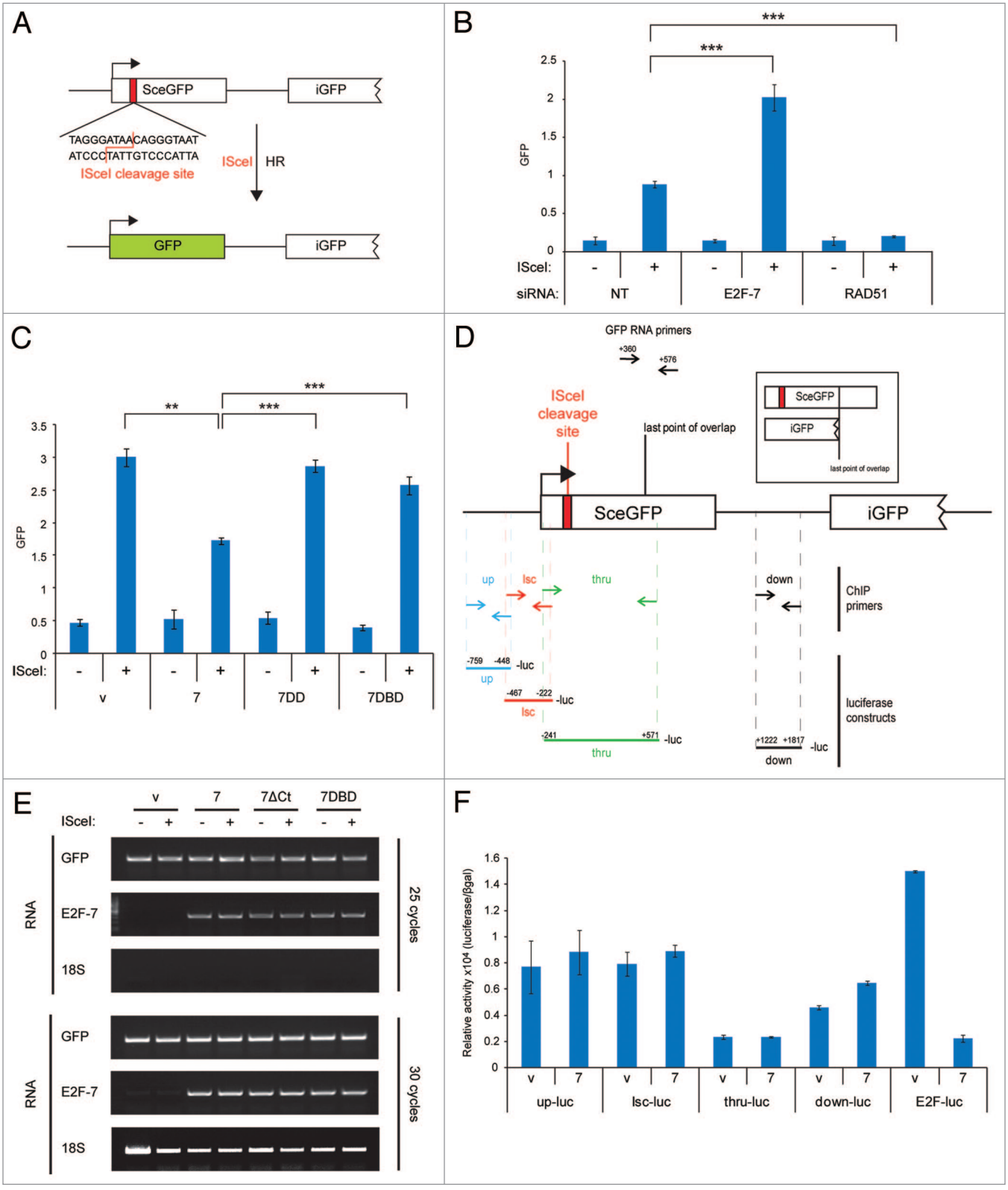

Figure 2. For figure legend, see page 3040.

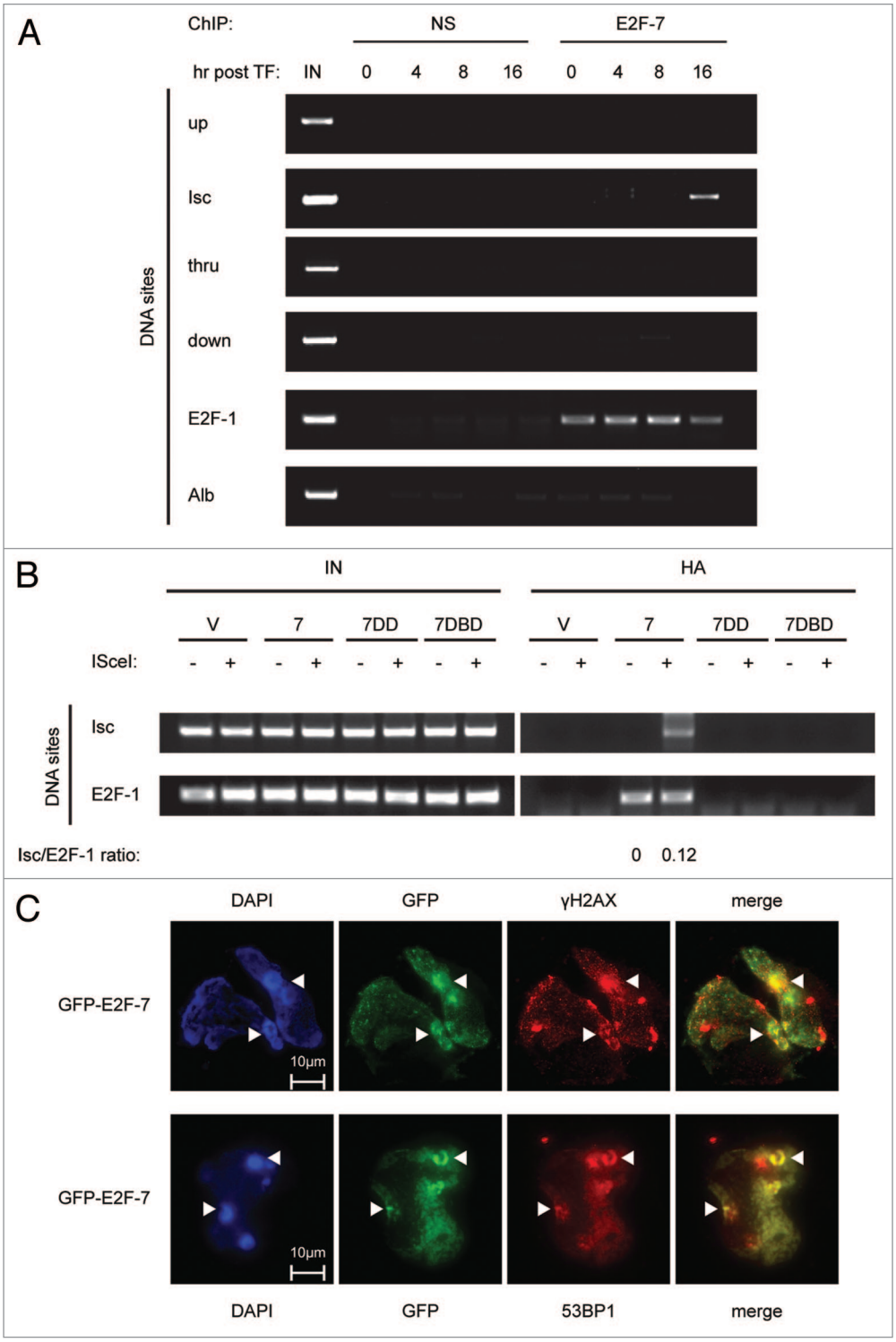

Figure 3A–C. E2F-7 localizes to DSBs and directly binds to damaged DNA. (**A**) Representative ChIP analysis on U2OS DR-GFP cells transfected with ISceI from 0 to 16 h, and immunoprecipitated with non-specific (NS) or E2F-7 antibody. The input chromatin (IN) is indicated. The E2F-1 promoter served as a positive control, Alb served as a negative control. (**B**) Representative ChIP analysis on U2OS DR-GFP cells transfected with control vector (–) or ISceI (+) and HA-E2F-7 (7), dimerization domain (7DD) or DNA-binding domain (7DBD mutants). Cell lysates were immunoprecipitated with anti-HA antibody. The input chromatin (IN) is indicated, and binding to the E2F binding sites in the E2F-1 promoter served as a positive control. Shown are the ratios of immunoprecipitated Isc DNA over E2F-1 DNA fragments. See also **Figure S3B**. (**C**) U2OS cells were transfected with GFP-E2F-7, treated with CPT (25 nM) for 24 h, and subjected to immunofluorescence. GFP (green) and γH2AX or 53BP1 (red) foci were analyzed for co-localization by a composite image (merged; yellow foci). Cell nuclei were counter-stained with DAPI.

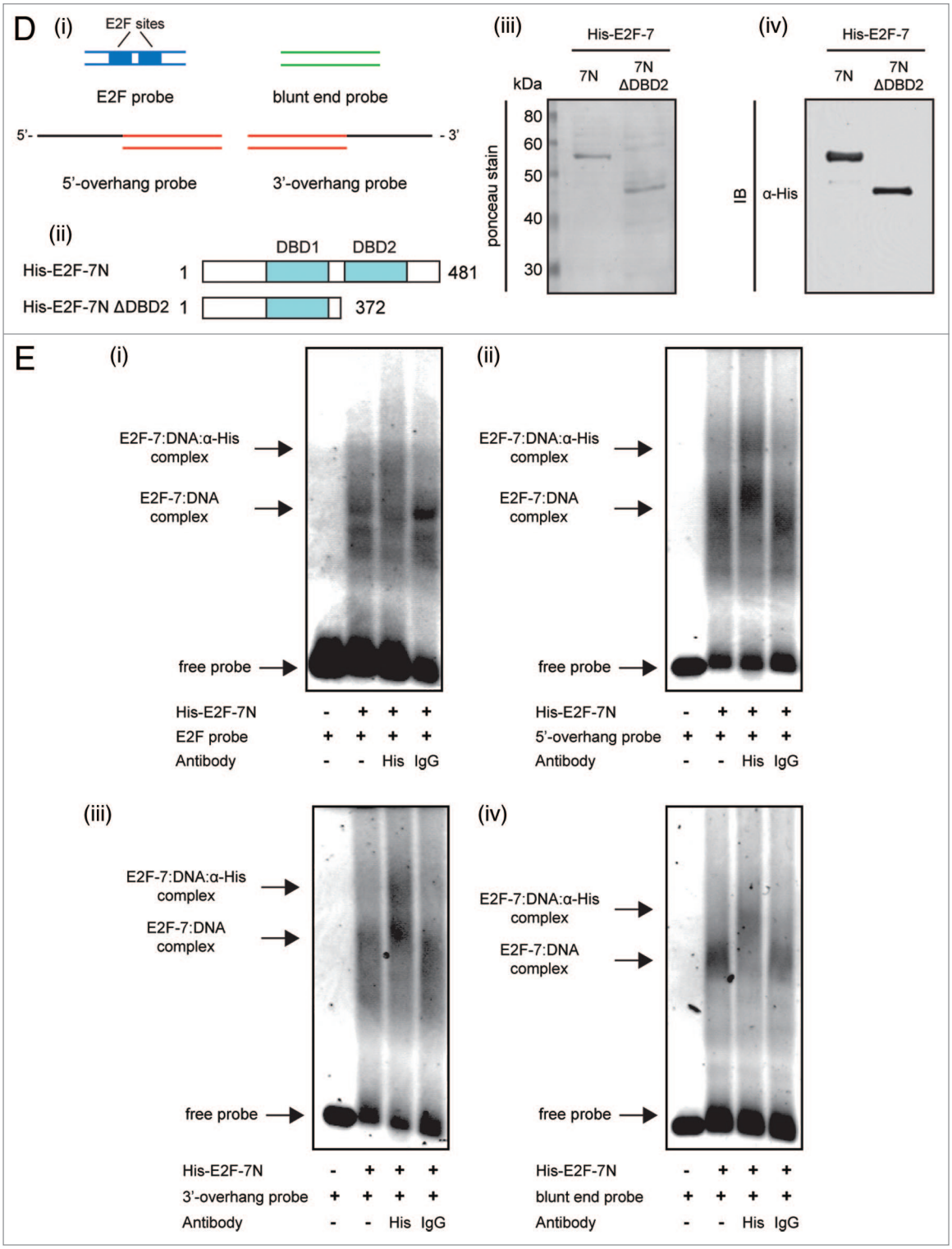

Figure 3D and E. (**D**, i) Schematic representation of the DNA probes: E2F (containing the E2F-1 promoter E2F sites: TTTCGCGGCAAAA and TTTGGCGCGTAAA), 5′ overhang, 3′ overhang and blunt end used for EMSAs; the E2F sites are indicated. Same colors (blue, green, red) represent complementarity between the oligonucleotides used to generate the double-stranded DNA probes. The black lines represent the DNA overhangs. (ii) Schematic representation of His-tagged E2F-7 proteins used for EMSAs. Indicated are the positions of the DNA binding domains (DBD) and expected size of the proteins. (iii) Input protein levels of His-tagged E2F-7 proteins (5 μg), as detected by Ponceau stain. The actual size (kDa) of the proteins is compared with proteins markers, as indicated. (iv) Input protein levels of His-tagged E2F-7 proteins (5 μg), as analyzed by immunoblot with anti-His. (**E**) His-E2F-7 (His-E2F-7N) was assessed for DNA binding by EMSA on the E2F (i) and DNA repair probes: 5′overhang (ii), 3′ overhang (iii) and blunt end (i). Reactions were run on 1% agarose gel in the presence of anti-His or control IgG (1 μg) and stained with EtBr. E2F-7: DNA, E2F-7: DNA: anti-His complexes and free DNA probe are indicated with arrows. See also **Figure S3C**.

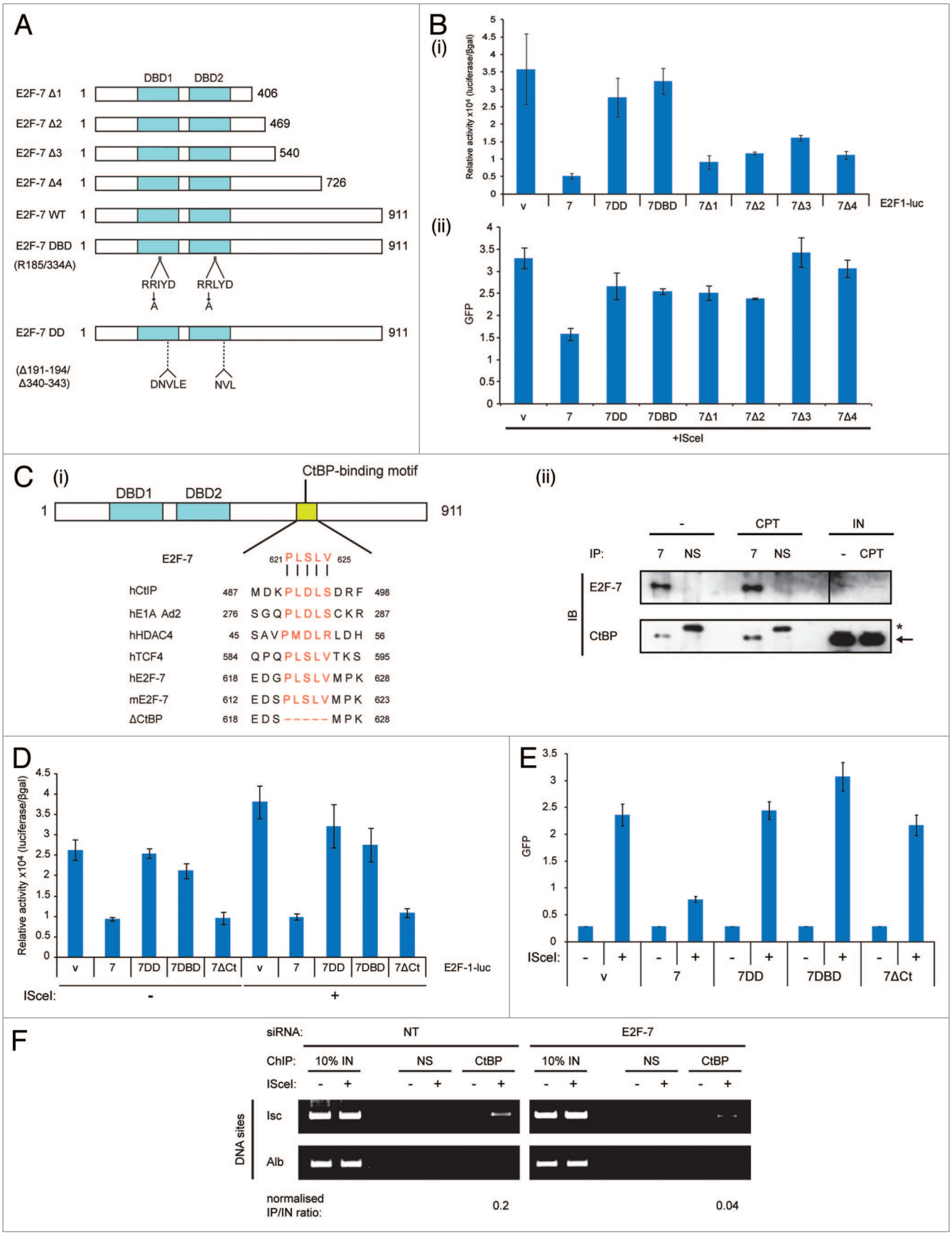

Figure 4. For figure legend, see page 3045.

activators bound to cognate DNA binding sites induce local chromatin remodeling (for example mediated by acetyl transferase) to facilitate DNA repair.[27] Moreover, it has become increasingly evident that the chromatin environment is altered in response to DSBs, which frequently involves proteins with established roles in chromatin modification and transcription.[28-30] In fact, we suggest that E2F-7 is a contributory factor recruited to chromatin in response to DSBs. There are established precedents for this idea, including histone-modifying enzymes and chromatin-modeling factors, many of which are known transcription regulators that become recruited to damaged DNA.[29,30] We would place E2F-7 and its associated chromatin modifiers in this category, rather than in a mechanistic effector group involved with DNA damage. We suggest that this is an attractive model, which fits with the data presented in the paper and the properties of E2F-7.

Tumor suppressor p53 provides notable example of a multifunctional transcription factor. Transcription-independent roles of p53 are known to control the efficiency of DNA repair and recombination.[31] For example, p53 directly interacts with proteins such as the TFIIH complex, which allows transcription to be coupled with nucleotide excision repair.[32] p53 also binds to the replication protein A complex which functions in DNA replication, HR, and NER.[33,34] It has been suggested that p53 can bind directly to damaged DNA, as it has short, single-stranded DNA binding activity and interacts directly with lesions in DNA.[35] In this respect, the properties of E2F-7 overlap considerably with p53; both proteins function in DNA damaged cells to limit cell cycle progression, in part by regulating an overlapping set of genes, but also influence the DNA repair process directly.

Of considerable importance is the evidence for somatic mutation in the E2F-7 gene in human cancer. These include not only a range of missense mutations, but also nonsense mutations that result in the expression of truncated E2F-7 proteins. Some of the mutant E2F-7 proteins had compromised transcription and DNA repair activity, particularly clear for the nonsense mutation (R288*, R333*, K423*, and L748*). The somatic mutation of the E2F-7 gene suggests that its mutation provides a survival advantage during tumorigenesis. Releasing the expression of E2F target genes, many of which are connected with cell cycle progression, and overcoming the negative impact of E2F-7 on HR (and thus perhaps augmenting the cellular mutation rate) are 2 possibilities that might explain the significance of E2F-7 mutation in cancer.

In conclusion, our study suggests that E2F-7 influences both transcriptional and non-transcriptional mechanisms in response to DNA damage. As such, E2F-7 allows coupling of transcription of many genes involved in DNA replication and repair directly with the mechanism of DNA repair, thus enabling cell cycle progression to be integrated with DNA repair.

Materials and Methods

Cell culture and transfection

Cells were cultured in Dulbecco modified Eagle medium (DMEM) supplemented with 5% (v/v) fetal calf serum (FCS), 100 U/ml penicillin, and 100 μg/ml streptomycin at 37 °C in a 5% CO_2 atmosphere. U2OS DR-GFP cells were supplemented with puromycin (1 μg/ml) to maintain stable expression of the DR-GFP cassette.[17] For DNA repair time-course experiments, cells were incubated with camptothecin (CPT) for 24 h, washed 3× with PBS and incubated with pre-warmed media, as indicated. Compounds were added at a 1:1000 dilution to minimize vehicle effects. Cells were transfected with 1–4 μg of total DNA at 30–50% confluency, using GeneJuice® (Merck). For short interfering RNA (siRNA)-mediated RNAi cells were transfected at 20–40% confluency with Oligofectamine (Invitrogen) and 21 bp oligonucleotides at 20–40 nM. Cells were routinely incubated with DNA/siRNA for 48–72 h. Untransfected and mock controls were routinely used and empty vector or NT#3 (Dharmacon) were used to equalize for the amount of DNA or siRNA, respectively, in the case of co-transfection.

Expression vectors and siRNA

Previously described vectors are: HA-E2F-7, HA-E2F-7DD, HA-E2F-7DBD, Flag-E2F-7, HA-E2F-1, pCMV-β-gal, pBB14-GFP and pE2F-luc,[12] and HA-ISceI.[17] The E2F-7 mutants E2F-7ΔCtBP and E2F-7Δ1, E2F-7Δ2, E2F-7Δ3, E2F-7Δ4 were generated by using Agilent's QuikChange Multi Site-Directed Mutagenesis kit. The up-, Isc-, thru-, down-luc vectors were generated by cloning PCR fragments amplified with the corresponding ChIP primers into pGL3-basic luciferase vector (Promega). The GFP-E2F-7 was sub-cloned into a pCMV-GFP construct. HA-HDAC1 and Flag-HDAC2 were cloned from cellular mRNA using standard techniques. His-tagged E2F-7N and His-tagged E2F-7N ΔDBD2 were kindly provided by Structural Genomics Consortium Oxford. The siRNA sequences used were: non-targeting 3 (NT#3), E2F-7 siRNA(i): AAAGGTACGA CGCCTCTATGA, E2F-7 siRNA(ii): AACAGAAGAG CGAGGTCGTAA, RAD51 siRNA (Dharmacon Smartpool) and E2F-1 siRNA1: ACTGACCATC AGTACCTGGUU; E2F-1 siRNA2: GAAGTCCAAG AACCACATCUU.

Figure 4 (See previous page). E2F-7 requires association with CtBP to regulate HR. (**A**) Schematic representation of the E2F-7 C-terminal deletion (Δ1-Δ4), DBD and DD mutants. The colored areas indicate the DNA binding domains. (**B**) (i) U2OS DR-GFP cells were transfected with ISceI and E2F-7 (7), 7DD, 7DBD or E2F-7 C-terminal deletion (Δ1-Δ4) mutants and E2F-1-luciferase reporter. Shown are the ratios of luciferase to β-gal activity. Error bars, SD (n = 3). Also see **Figure S4A**. (ii) U2OS DR-GFP cells were transfected with ISceI (ISceI) and the E2F-7 mutant derivatives. Shown are the normalized GFP levels. Error bars, SD (n = 3). (**C**) (i) Schematic representation of the E2F-7ΔCtBP mutant and sequence alignment of CtBP-binding motifs in CtBP interacting proteins and human (h) and mouse (m) E2F-7. (ii) Hela cells were treated with CPT (25 nM) for 16 h, or left untreated, endogenous E2F-7 was immunoprecipitated from lysates and immunoblotted, as indicated. CtBP is indicated by arrow, asterisk indicates non-specific polypeptide. (**D**) U2OS DR-GFP cells were transfected with control vector (–) or ISceI (+) and E2F-7 (7), 7DD, 7DBD, or 7ΔCt and E2F-1-luciferase reporter construct. Shown are the ratios of luciferase to β-gal activity. Error bars, SD (n = 3). See also **Figure S4C**. (**E**) U2OS DR-GFP cells were co-transfected with control vector (–) or ISceI (+) and E2F-7 (7), 7DD, 7DBD, or 7ΔCt. Shown are the normalized GFP levels. Error bars, SD (n = 3). See also **Figure S4D**. (**F**) Representative ChIP analysis on U2OS DR-GFP cells transfected with NT or E2F-7 siRNA, control vector (–) or ISceI (+) for 16 h and immunoprecipitated with NS or CtBP antibody. The input chromatin (IN) is indicated, Alb served as a negative control. Shown are the ratios of immunoprecipitated DNA over input, and normalized to input levels. Also see **Figure S4E**.

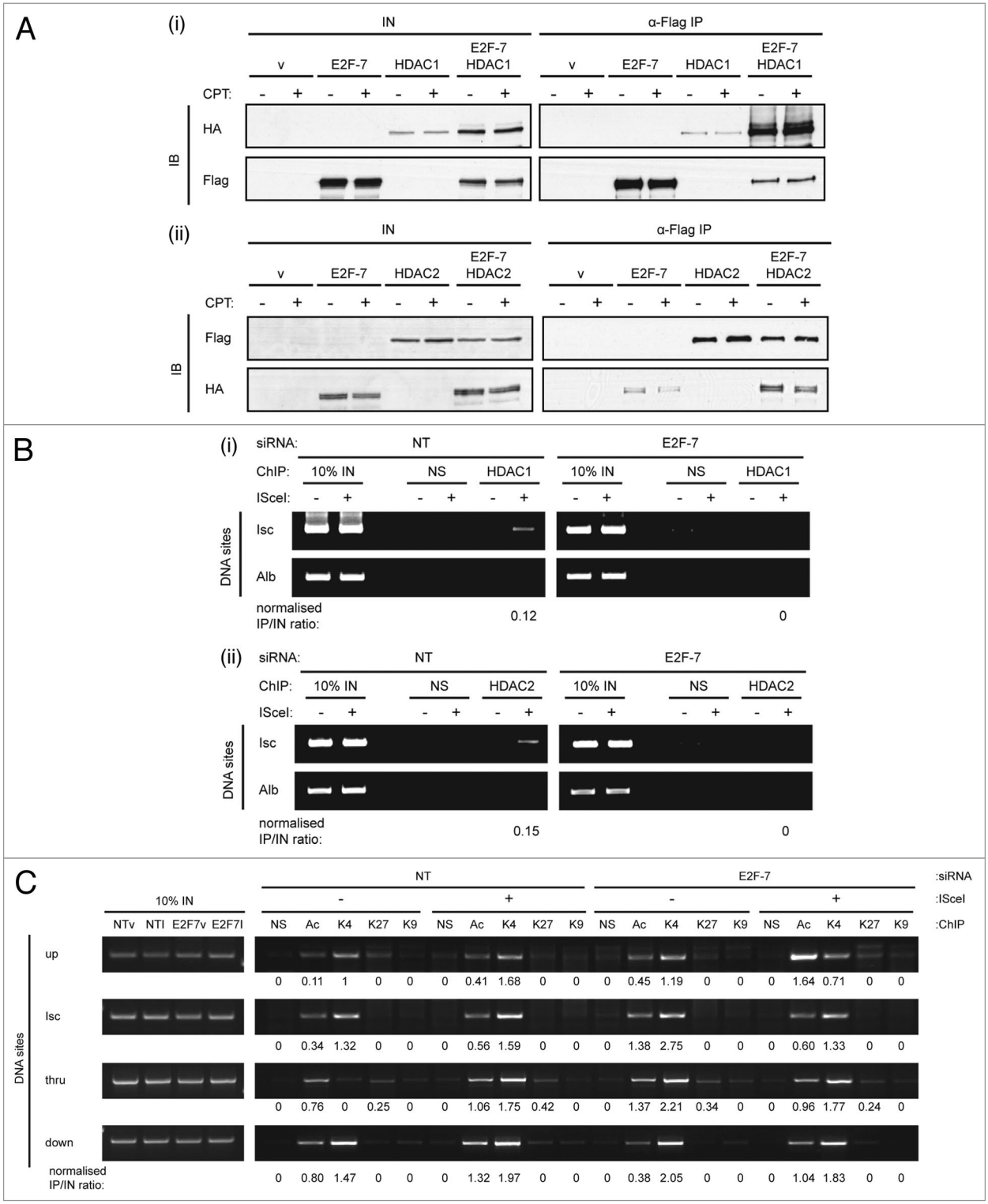

Figure 5. E2F-7 interacts with HDACs and alters the local chromatin environment of the DSB. (**A**) (i) U2OS cells were transfected with Flag-tagged E2F-7 or HA-tagged HDAC1 or both and treated with camptothecin (CPT +; 25 nM) for 16 h or left untreated (–). Lysates were immunoprecipitated with anti-Flag and immunoblotted with anti-HA. (ii) U2OS cells were transfected with HA-tagged E2F-7 or Flag-tagged HDAC2 or both and treated with camptothecin (CPT +; 25 nM) for 16 h or left untreated (–). Lysates were immunoprecipitated with anti-Flag and immunoblotted with anti-HA. (**B**) Representative ChIP analyses on U2OS DR-GFP cells transfected with NT or E2F-7 siRNA, control vector (–) or ISceI (+) for 16 h and immunoprecipitated with NS or HDAC1 (i) or HDAC2 (ii) antibodies. The input chromatin (IN) is indicated, Alb served as a negative control. Shown are the ratios of immunoprecipitated DNA over input, and normalized to input levels. Also see **Figure S4F**. (**C**) (i) Representative ChIP analysis from U2OS DR-GFP cells treated with NT or E2F-7 siRNA, subsequently transfected with control vector (–) or HA-ISceI (+) for 16 h and immunoprecipitated with non-specific (IgG) or acetylated histone 3 (Ac), trimethylated lysine 4 histone 3 (K4), trimethylated lysine 27 histone 3 (K27), or trimethylated lysine 9 histone 3 (K9) antibody. The input (IN) chromatin is indicated. Shown are the ratios of immunoprecipitated DNA over input, and normalized to input levels for each PCR fragment. Also see **Figure S4F**.

Reverse-transcriptase polymerase chain reaction

RNA was extracted using the Trizol reagent (Invitrogen), according to the manufacturer's protocol. cDNA was synthesized from total RNA using the MMLV system (Promega) and the target cDNA was amplified by polymerase chain reaction (PCR) using primers pairs E2F-7, 18S[12] and GFP Fwd: 5′-TATATCATGG CCGACA -3′, GFP Rev 5′- ACATGGTCCT GCTGGAGTTC -3′. The PCR reaction was as follows: 95 °C for 5 min, 25 or 30 cycles of 95 °C for 30 s, 58 °C for 1 min, 72 °C for 1 min, and 72 °C for 5 min. PCR products were run on 2% agarose gel containing 0.5 μg/ml ethidium bromide and visualized under UV.

Protein extraction, SDS-PAGE, and immunoblotting

Cells were lysed either in TNN lysis buffer (50 mM Tris-Cl pH 7.5, 5 mM ethylene diamine tetra-acetic acid [EDTA] pH 8.0, 200 mM NaCl, 0.5% Igepal CA-360, 10 mM NaF, 1 mM

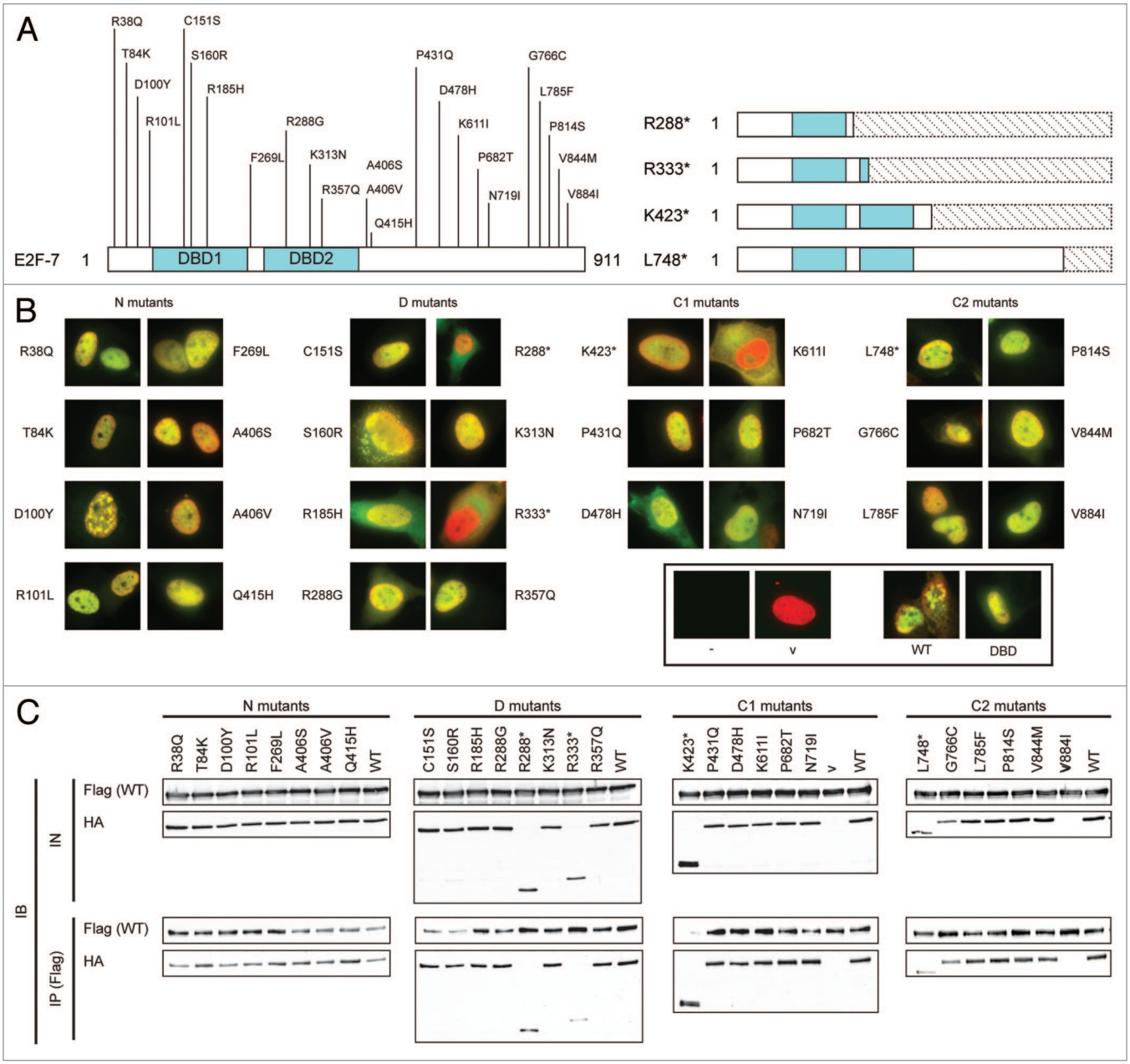

Figure 6A–C. Tumor derived mutants have compromised transcription and DNA repair properties. (**A**) Schematic representation of E2F-7, indicating the location of the mutations identified from the COSMIC database. Shown are 28 point mutations, of which 24 are missense and 4 are nonsense, as indicated, which are confirmed somatic by comparison to matched (non-tumor) germline DNA (http://cancer.sanger.ac.uk/cancergenome/projects/cosmic/). For clarity, the mutant derivatives of E2F-7 were categorized based on their position on the E2F-7 protein, in N-terminal (N), DNA binding domain (D), C-terminal (C1), and C-terminal tail (C2). (**B**) U2OS cells were transfected with HA-E2F-7 mutant derivatives together with Flag-E2F-7 WT, as indicated, and protein localization was assessed by indirect immunofluorescence with anti-HA and anti-Flag. Protein co-localization is shown in yellow. (**C**) U2OS cells were transfected with Flag-E2F-7 WT and HA-E2F-7 mutant derivatives, as indicated. Cell lysates were immunoprecipitated with anti-Flag, followed by immunoblotting with anti-HA (mutant derivatives) and anti-Flag (E2F-7 WT).

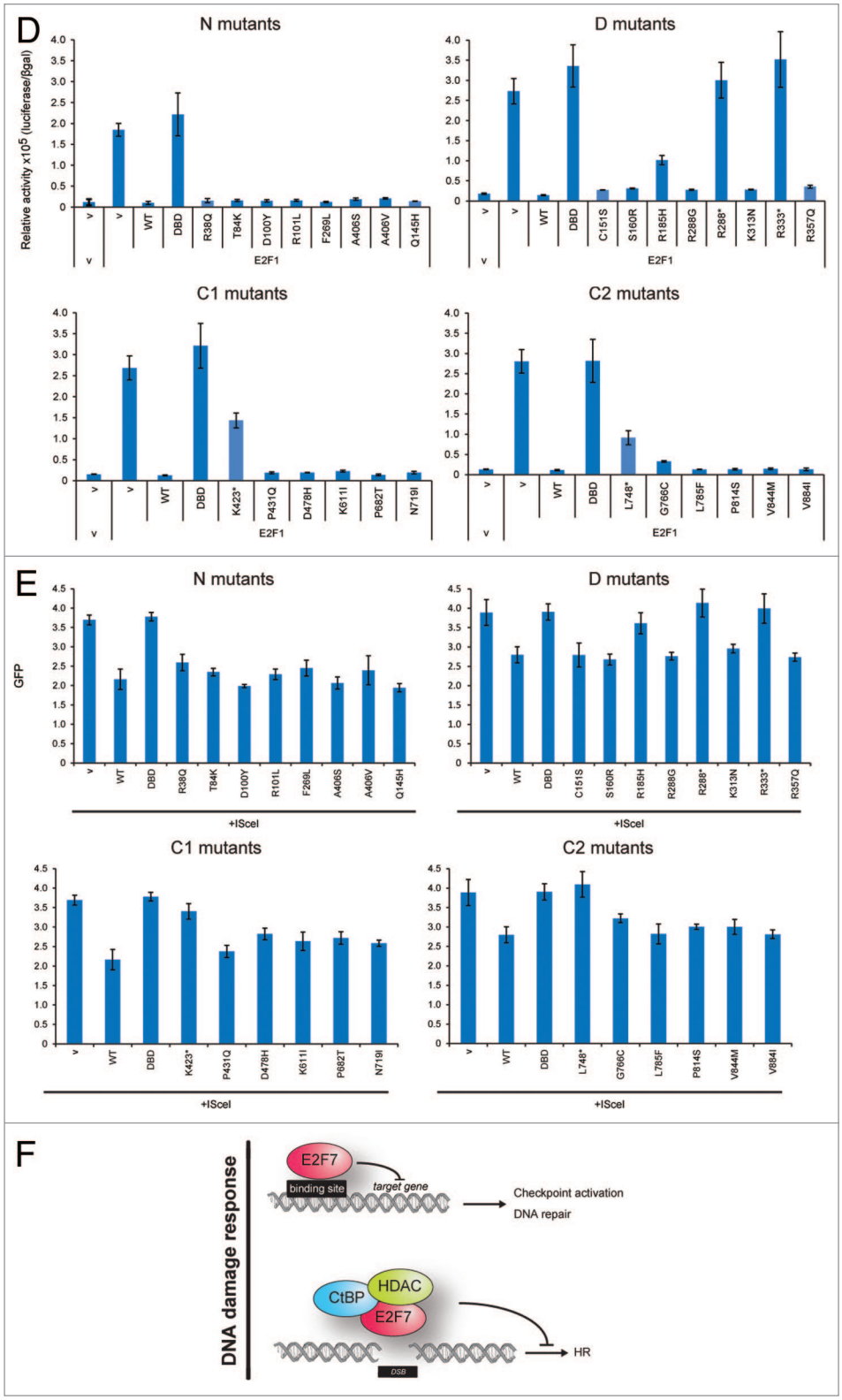

Figure 6D–F. (**D**) U2OS cells were transfected with control vector (v) or E2F-7 mutant derivatives, as indicated, together with HA-E2F-1, E2F-1-luciferase reporter construct and CMV-β-gal (as the internal control for transfection efficiency). The results represent the ratio of luciferase to β-gal activity. Error bars, SD (n = 3). Also see **Figure S5A**. (**E**) U2OS DR-GFP cells were transfected with control vector (v) or HA-ISceI endonuclease (I) and the E2F-7 mutant derivatives, as indicated. The results represent the level of GFP intensity as measured by flow cytometry. Error bars, SD (n = 3). Also see **Figure S5B**. (**F**) Proposed model for E2F-7 mechanism of action during the DNA repair process. In addition to the role of E2F-7 as a transcriptional regulator, E2F-7 locates to areas of DNA damage, such as a DSB, recruiting histone modifiers like HDAC. This allows E2F-7 to act on the chromatin environment of the damaged DNA. It is possible that this property of E2F-7 is relevant in checkpoint activation and DNA repair processes that occur upon DNA damage.

Na_3VO_4, and protease inhibitor [PI] cocktail) on ice for 30 min. Protein concentration was measured using the Bradford method (BioRad). Standard SDS-PAGE electrophoresis and immunoblotting protocols were followed; visualization was performed by enhanced chemiluminescence (ECL) and exposure of membranes to X-ray Film (Kodak).

Antibodies

The antibodies used were: E2F-7 N-20 (Santa Cruz), E2F-1 KH-95 (Santa Cruz) GAPDH V-18 (Santa Cruz), γH2AX 05–636 (Millipore), H2AX ab20669 (Abcam), RAD51 H-92 (Santa Cruz), 53BP1 (Bethyl Laboratories), HA-11 (Gibco), CtBP E-12 (Santa Cruz), Flag M2 (Sigma), HDAC1 H-11 (Santa Cruz), HDAC2 H-54 (Santa Cruz), acetyl-H3 06–599 (Millipore), H3K4me3 ab8580 (Abcam), H3K9me3 07–442 (Millipore), H3K27me3 ab24684 (Abcam), FITC-conjugated BrdU 556028 (BD Biosciences), His H1029 (Sigma), and control immunoglobulins (IgG) (GE Healthcare) .

Luciferase reporter assay

Cells were transfected with pE2F1-luc (0.5 μg) and pCMVβ-gal (0.5 μg) as an internal control as previously described.[36] Twenty-four–36 h after transfection, cells were harvested and used for luciferase and β-galactosidase activity assays. All assays were performed in triplicate and were normalized relative to β-galactosidase activity.

Immunoprecipitation

Cells were washed in PBS and lysed in reduced NaCl (150 mM) TNN buffer. Lysates were incubated overnight at 4 °C with 20 μl HA-agarose (Sigma) or Flag-agarose for ectopic IPs or 2 μg of E2F-7 and 20 μl protein A/G beads. Beads were washed 4× with TNN followed by protein elution with 2× SDS loading buffer; analysis was by SDS PAGE and immunoblotting. Band intensities were quantified by Image J.

Immunofluorescence

Cells were seeded on coverslips and 48 h after transfection with siRNA were subjected to treatments, as indicated. Coverslips were subsequently washed in 1× PBS and fixed with 3.7% formaldehyde in PBS with 1% Triton X-100 for 15 min, permeabilized in 0.5% Triton X-100 in PBS for 5 min, and incubated with specific antibodies, as indicated. Coverslips were then washed in 3× PBS 0.05% Tween-20 and subsequently incubated with fluorescently labeled secondary antibodies (Alexa, Invitrogen) and mounted onto microscope slides using DAPI Vectashield mounting media (Vector labs). Protein localization was then visualized using a BX60 transmitted-reflective light fluorescence microscope (Olympus) and data was analyzed using OpenLab software (Improvision).

UV light-induced microirradiation

UV induced microirradiation, as previously described.[19] Briefly, cells were seeded on coverslips and 24 h after DNA transfection, 10 μM BrdU (BD Biosciences) was added to the media for an additional 48 h. Prior to UV irradiation, the culture medium was removed, and coveslips were washed with PBS. Immediately after removal of PBS, coverslips were covered with a micropore membrane (Isopore 5 μM, Millipore) and exposed to 30 J/m^2 UV in a UV crosslinker (GE Healthcare). After exposure, cells were replenished with culture medium and incubated at 37 °C in a CO_2 incubator for 30 min. Coverslips were subjected to immunofluorescence, as described above.

Flow cytometry of cell cycle distribution and BrdU incorporation

For propidium iodide (PI) staining cells were harvested in Trypsin-EDTA (Lonza) until they detached from the plates, followed by addition of 5% FCS in DMEM. Cells were washed with PBS, fixed by addition of 1 ml of ice-cold 50% ethanol/PBS and resuspended in 25 U/ml RNaseA (Sigma) and 50 μg/ml propidium iodide (PI) (Sigma) and incubated for 30 min on ice in the dark. Cells were collected on an Accuri C6 flow cytometer (Becton-Dickinson) and analyzed using the Accuri CFlow (Becton-Dickinson). In the case of BrdU incorporation, BrdU (BD Biosciences) was added to cells at 10 μM, as indicated, and cells were stained with anti-BrdU (Becton-Dickinson) and PI, according to the manufacturer's protocol.

Homologous recombination assay

HR-dependent DNA DSB repair was assessed using the DR-GFP/ISceI assay, as previously described.[18] Briefly, cells were transfected with 1 μg HA-ISceI, unless otherwise indicated, and incubated for a minimum of 48 h. Cells were harvested, washed, resuspended in PBS, and analyzed for GFP expression on the Accuri C6 flow cytometer. In siRNA experiments, cells were treated with siRNA for 48 h, trypsinized, and allowed to replate before DNA transfection. In ectopic expression experiments, DNA was co-tranfected with HA-ISceI for the same length of time. To rule out differences in transfection efficiency, the transfection efficiency of HR assays was measured by parallel transfection of pCMV-GFP instead of HA-ISceI, as previously described.[37,38] The DR-GFP fluorescence data are presented as the absolute percentage of GFP-expressing cells normalized for transfection efficiency by generating transfection efficiency ratios to the control non-ISceI treatment and subsequently normalizing all other treatments accordingly. The corresponding input protein levels were loaded on total protein content and are, therefore, indicative of ectopic protein expression, without reflecting transfection efficiency for each sample.

Electrophoretic mobility shift assays

Oligonucleotides were synthesized and purified by PAGE (PAGE) by SIGMA Genosys. The following oligonucleotides were used: E2F-1 F ′-GGCTCTTTCG CGGCAAAAAG GATTTGGCGC GTAAAAGTGG -3′); E2F-1 R (5′-CCACTTTTAC GCGCCAAATC CTTTTTGCCG CGAAAGAGCC -3′); Repair-5′ F (5′-ATTTACTTAT TTTGTATTAT CCTTATTTAT ATCCTTTCTG CTTTATCAAG ATAATTTTTC GACTCATCAG AAATATCCG-3′); Repair-3′F (CTGCTTTATC AAGATAATT TTTCGACTCA TCAGAAATAT CCGTTTCCTA TATTTATTCC TATTATGTTT TATTCATTTA); Repair R (5′- CGGATATTTC TGATGAGTCG AAAAATTATC TTGATAAAGC AG-3′); Repair blunt end F (5′-TAATACAAAAT AAGTAAATGA ATAAACAGAGAA AATAAAG-3′); Repair blunt end R (5′-CTTTATTTTC TCTGTTTATT CATTTACTT ATTTTGTATTA-3′). To generate the different double-stranded DNA probes, oligonucleotides were annealed at a 1:1 molar ratio

in annealing buffer (100 mM Tris-Cl pH 7.6, 10 mM DTT, 20 mM $MgCl_2$, 2 mM Spermidine) as follows: E2F-1 F and R for the E2F probe (40-mer), repair 5′ F and repair R for the 5′ overhang probe (79-mer with 42 nt in double strand and 37 nt 5′ overhang), repair 3′ F and repair R for the 3′ overhang probe (79-mer with 42 nt in double strand and 37 nt 3′ overhang), and repair blunt end F and R for the BE probe (40-mer). Repair oligonucleotides were modified from[39] to generate probes of similar length to E2F-1. Bacterially expressed and purified His-E2F-7N and His-E2F-N ΔDBD2 were incubated with 500 μg of double-stranded DNA substrate for 20 min at RT in 1× EMSA binding buffer (400 mM KCl, 150 mM Hepes pH 7.9, 10 mM EDTA, 5 mM DTT, 50% glycerol). For supershift, protein was pre-incubated with anti-His or IgG for 10 min at RT before DNA was added for 20 min. Where indicated, proteins were denatured by incubation at 95 °C for 10 min. The reactions were resolved by electrophoresis on a 1% agarose gel in TAE (40 mM Tris-acetate pH 7.5, 0.5 mM EDTA) buffer for 1 h at 100 mAmp. The gel was then stained in 1xTAE buffer containing EtBr at 0.5 μg/ml for 15 min and visualized under UV.

Chromatin immunoprecipitation

Chromatin immunoprecipitations were performed as described.[12] For DR-GPF ChIPs, cells were transfected with HA-ISceI plasmid at the indicated concentrations and cells were routinely harvested for ChIP 16–24 h post-transfection unless otherwise indicated. For siRNA DR-GFP ChIPs cells were treated with siRNA for 72 h, trypsinized, and allowed to re-plate before transfection with DNA. DNA was amplified with Paq5000 polymerase (Agilent) with specific primers pairs for promoter regions of E2F-1, Alb[12]; DR-GFP primers (up, Isc, thru, down) designed to amplify regions the DR-GFP cassette, as indicated. Primer sequences are available upon request. PCR settings were as follows: 95 °C for 3 min, 32 cycles of 95 °C for 30 s, 61 °C for 1 min, and 72 °C for 1 min, and 72 °C for 5 min. Products were visualized on 2% agarose gel with 0.5 μg/ml ethidium bromide. Band intensities were quantified by ImageJ.

Analysis of human tumor derived mutations of E2F-7

The Catalogue of Somatic Mutations in Cancer (COSMIC) database (http://www.sanger.ac.uk/genetics/CGP/cosmic/)[40] was interrogated for mutations of E2F-7 (NM_203394.2) in human tumor samples. At the point of submission, 42 simple mutations were identified from 348 samples analyzed. The majority of these mutations were missense (28) and nonsense (4); 9 synonymous mutations were also identified. For the mutations selected for further analysis, corresponding HA-E2F-7 constructs were generated by using Agilent's QuikChange Multi Site-Directed Mutagenesis kit with specific primers introducing a substitution at the desired positions.

Disclosure of Potential Conflicts of Interest

No potential conflicts of interest were disclosed.

Acknowledgments

This work was supported by grants from CRUK (program award C300/A13058) and MRC. We thank Sarah Atkinson for help with the manuscript preparation.

Author Contributions

LZ planned and performed the majority of experiments and data analysis. AC planned, performed and analyzed additional experiments. TH provided materials and advice. NLT wrote the manuscript and directed the project.

Supplemental Materials

Supplemental materials may be found here:
www.landesbioscience.com/journals/cc/article/26078

References

1. Jeggo PA, Löbrich M. DNA double-strand breaks: their cellular and clinical impact? Oncogene 2007; 26:7717-9; PMID:18066083; http://dx.doi.org/10.1038/sj.onc.1210868
2. Koundrioukoff S, Polo S, Almouzni G. Interplay between chromatin and cell cycle checkpoints in the context of ATR/ATM-dependent checkpoints. DNA Repair (Amst) 2004; 3:969-78; PMID:15279783; http://dx.doi.org/10.1016/j.dnarep.2004.03.010
3. Kasparek TR, Humphrey TC. DNA double-strand break repair pathways, chromosomal rearrangements and cancer. Semin Cell Dev Biol 2011; 22:886-97; PMID:22027614; http://dx.doi.org/10.1016/j.semcdb.2011.10.007
4. Rogakou EP, Pilch DR, Orr AH, Ivanova VS, Bonner WM. DNA double-stranded breaks induce histone H2AX phosphorylation on serine 139. J Biol Chem 1998; 273:5858-68; PMID:9488723; http://dx.doi.org/10.1074/jbc.273.10.5858
5. Longhese MP, Bonetti D, Manfrini N, Clerici M. Mechanisms and regulation of DNA end resection. EMBO J 2010; 29:2864-74; PMID:20647996; http://dx.doi.org/10.1038/emboj.2010.165
6. Chen HZ, Tsai SY, Leone G. Emerging roles of E2Fs in cancer: an exit from cell cycle control. Nat Rev Cancer 2009; 9:785-97; PMID:19851314; http://dx.doi.org/10.1038/nrc2696
7. Bandara LR, La Thangue NB. Adenovirus E1a prevents the retinoblastoma gene product from complexing with a cellular transcription factor. Nature 1991; 351:494-7; PMID:1710781; http://dx.doi.org/10.1038/351494a0
8. Weinberg RA. The retinoblastoma protein and cell cycle control. Cell 1995; 81:323-30; PMID:7736585; http://dx.doi.org/10.1016/0092-8674(95)90385-2
9. Logan N, Delavaine L, Graham A, Reilly C, Wilson J, Brummelkamp TR, Hijmans EM, Bernards R, La Thangue NB. E2F-7: a distinctive E2F family member with an unusual organization of DNA-binding domains. Oncogene 2004; 23:5138-50; PMID:15133492; http://dx.doi.org/10.1038/sj.onc.1207649
10. Di Stefano L, Jensen MR, Helin K. E2F7, a novel E2F featuring DP-independent repression of a subset of E2F-regulated genes. EMBO J 2003; 22:6289-98; PMID:14633988; http://dx.doi.org/10.1093/emboj/cdg613
11. de Bruin A, Maiti B, Jakoi L, Timmers C, Buerki R, Leone G. Identification and characterization of E2F7, a novel mammalian E2F family member capable of blocking cellular proliferation. J Biol Chem 2003; 278:42041-9; PMID:12893818; http://dx.doi.org/10.1074/jbc.M308105200
12. Zalmas LP, Zhao X, Graham AL, Fisher R, Reilly C, Coutts AS, La Thangue NB. DNA-damage response control of E2F7 and E2F8. EMBO Rep 2008; 9:252-9; PMID:18202719; http://dx.doi.org/10.1038/sj.embor.7401158
13. Clements MK, Jones CB, Cumming M, Daoud SS. Antiangiogenic potential of camptothecin and topotecan. Cancer Chemother Pharmacol 1999; 44:411-6; PMID:10501915; http://dx.doi.org/10.1007/s002800050997
14. Costa-Pereira AP, McKenna SL, Cotter TG. Activation of SAPK/JNK by camptothecin sensitizes androgen-independent prostate cancer cells to Fas-induced apoptosis. Br J Cancer 2000; 82:1827-34; PMID:10839298; http://dx.doi.org/10.1054/bjoc.2000.1149
15. Pommier Y, Redon C, Rao VA, Seiler JA, Sordet O, Takemura H, Antony S, Meng L, Liao Z, Kohlhagen G, et al. Repair of and checkpoint response to topoisomerase I-mediated DNA damage. Mutat Res 2003; 532:173-203; PMID:14643436; http://dx.doi.org/10.1016/j.mrfmmm.2003.08.016
16. Heyer WD, Ehmsen KT, Liu J. Regulation of homologous recombination in eukaryotes. Annu Rev Genet 2010; 44:113-39; PMID:20690856; http://dx.doi.org/10.1146/annurev-genet-051710-150955
17. Gottipati P, Vischioni B, Schultz N, Solomons J, Bryant HE, Djureinovic T, Issaeva N, Sleeth K, Sharma RA, Helleday T. Poly(ADP-ribose) polymerase is hyperactivated in homologous recombination-defective cells. Cancer Res 2010; 70:5389-98; PMID:20551068; http://dx.doi.org/10.1158/0008-5472.CAN-09-4716

18. Boichuk S, Hu L, Makielski K, Pandolfi PP, Gjoerup OV. Functional connection between Rad51 and PML in homology-directed repair. PLoS One 2011; 6:e25814; PMID:21998700; http://dx.doi.org/10.1371/journal.pone.0025814
19. Suzuki K, Yamauchi M, Oka Y, Suzuki M, Yamashita S. Creating localized DNA double-strand breaks with microirradiation. Nat Protoc 2011; 6:134-9; PMID:21293454; http://dx.doi.org/10.1038/nprot.2010.183
20. Becherel OJ, Jakob B, Cherry AL, Gueven N, Fusser M, Kijas AW, Peng C, Katyal S, McKinnon PJ, Chen J, et al. CK2 phosphorylation-dependent interaction between aprataxin and MDC1 in the DNA damage response. Nucleic Acids Res 2010; 38:1489-503; PMID:20008512; http://dx.doi.org/10.1093/nar/gkp1149
21. Das BB, Antony S, Gupta S, Dexheimer TS, Redon CE, Garfield S, Shiloh Y, Pommier Y. Optimal function of the DNA repair enzyme TDP1 requires its phosphorylation by ATM and/or DNA-PK. EMBO J 2009; 28:3667-80; PMID:19851285; http://dx.doi.org/10.1038/emboj.2009.302
22. Li DQ, Nair SS, Ohshiro K, Kumar A, Nair VS, Pakala SB, Reddy SD, Gajula RP, Eswaran J, Aravind L, et al. MORC2 signaling integrates phosphorylation-dependent, ATPase-coupled chromatin remodeling during the DNA damage response. Cell Rep 2012; 2:1657-69; PMID:23260667; http://dx.doi.org/10.1016/j.celrep.2012.11.018
23. Symington LS, Gautier J. Double-strand break end resection and repair pathway choice. Annu Rev Genet 2011; 45:247-71; PMID:21910633; http://dx.doi.org/10.1146/annurev-genet-110410-132435
24. Subramanian T, Chinnadurai G. Association of class I histone deacetylases with transcriptional corepressor CtBP. FEBS Lett 2003; 540:255-8; PMID:12681518; http://dx.doi.org/10.1016/S0014-5793(03)00275-8
25. Sundqvist A, Sollerbrant K, Svensson C. The carboxy-terminal region of adenovirus E1A activates transcription through targeting of a C-terminal binding protein-histone deacetylase complex. FEBS Lett 1998; 429:183-8; PMID:9650586; http://dx.doi.org/10.1016/S0014-5793(98)00588-2
26. Drapkin R, Reardon JT, Ansari A, Huang JC, Zawel L, Ahn K, Sancar A, Reinberg D. Dual role of TFIIH in DNA excision repair and in transcription by RNA polymerase II. Nature 1994; 368:769-72; PMID:8152490; http://dx.doi.org/10.1038/368769a0
27. Rubbi CP, Milner J. p53 is a chromatin accessibility factor for nucleotide excision repair of DNA damage. EMBO J 2003; 22:975-86; PMID:12574133; http://dx.doi.org/10.1093/emboj/cdg082
28. Xu Y, Price BD. Chromatin dynamics and the repair of DNA double strand breaks. Cell Cycle 2011; 10:261-7; PMID:21212734; http://dx.doi.org/10.4161/cc.10.2.14543
29. Lukas J, Lukas C, Bartek J. More than just a focus: The chromatin response to DNA damage and its role in genome integrity maintenance. Nat Cell Biol 2011; 13:1161-9; PMID:21968989; http://dx.doi.org/10.1038/ncb2344
30. Polo SE, Jackson SP. Dynamics of DNA damage response proteins at DNA breaks: a focus on protein modifications. Genes Dev 2011; 25:409-33; PMID:21363960; http://dx.doi.org/10.1101/gad.2021311
31. Sengupta S, Harris CC. p53: traffic cop at the crossroads of DNA repair and recombination. Nat Rev Mol Cell Biol 2005; 6:44-55; PMID:15688066; http://dx.doi.org/10.1038/nrm1546
32. Wang QE, Zhu Q, Wani MA, Wani G, Chen J, Wani AA. Tumor suppressor p53 dependent recruitment of nucleotide excision repair factors XPC and TFIIH to DNA damage. DNA Repair (Amst) 2003; 2:483-99; PMID:12713809; http://dx.doi.org/10.1016/S1568-7864(03)00002-8
33. Romanova LY, Willers H, Blagosklonny MV, Powell SN. The interaction of p53 with replication protein A mediates suppression of homologous recombination. Oncogene 2004; 23:9025-33; PMID:15489903; http://dx.doi.org/10.1038/sj.onc.1207982
34. Riva F, Zuco V, Vink AA, Supino R, Prosperi E. UV-induced DNA incision and proliferating cell nuclear antigen recruitment to repair sites occur independently of p53-replication protein A interaction in p53 wild type and mutant ovarian carcinoma cells. Carcinogenesis 2001; 22:1971-8; PMID:11751427; http://dx.doi.org/10.1093/carcin/22.12.1971
35. Bakalkin G, Yakovleva T, Selivanova G, Magnusson KP, Szekely L, Kiseleva E, Klein G, Terenius L, Wiman KG. p53 binds single-stranded DNA ends and catalyzes DNA renaturation and strand transfer. Proc Natl Acad Sci U S A 1994; 91:413-7; PMID:8278402; http://dx.doi.org/10.1073/pnas.91.1.413
36. Logan N, Graham A, Zhao X, Fisher R, Maiti B, Leone G, La Thangue NB. E2F-8: an E2F family member with a similar organization of DNA-binding domains to E2F-7. Oncogene 2005; 24:5000-4; PMID:15897886; http://dx.doi.org/10.1038/sj.onc.1208703
37. Pierce AJ, Hu P, Han M, Ellis N, Jasin M. Ku DNA end-binding protein modulates homologous repair of double-strand breaks in mammalian cells. Genes Dev 2001; 15:3237-42; PMID:11751629; http://dx.doi.org/10.1101/gad.946401
38. Yang YG, Saidi A, Frappart PO, Min W, Barrucand C, Dumon-Jones V, Michelon J, Herceg Z, Wang ZQ. Conditional deletion of Nbs1 in murine cells reveals its role in branching repair pathways of DNA double-strand breaks. EMBO J 2006; 25:5527-38; PMID:17082765; http://dx.doi.org/10.1038/sj.emboj.7601411
39. Jensen RB, Carreira A, Kowalczykowski SC. Purified human BRCA2 stimulates RAD51-mediated recombination. Nature 2010; 467:678-83; PMID:20729832; http://dx.doi.org/10.1038/nature09399
40. Bamford S, Dawson E, Forbes S, Clements J, Pettett R, Dogan A, Flanagan A, Teague J, Futreal PA, Stratton MR, et al. The COSMIC (Catalogue of Somatic Mutations in Cancer) database and website. Br J Cancer 2004; 91:355-8; PMID:15188009